Characteristic Basis Function Analysis of Large Aperture-Fed Antenna Arrays

Context

- Irregular Sparse Antenna Arrays
- Gap Waveguide Antennas

Rob Maaskant, Carlo Bencivenni, and Marianna Ivashina

Antenna Group, Department of Signals and Systems
Chalmers University of Technology
S-41296 Gothenburg, Sweden
rob.maaskant@chalmers.se

EUCAP 2014, Den Haag, Nederland

CHALMERS
Chalmers University of Technology, Sweden

Outline

- Aperture Fed Antenna Arrays
  - Irregular Antenna Arrays
  - Gap Waveguide Antennas
- Generalized Admittance Matrix Approach
- Numerical Examples
- Conclusions

Area description
Large sparse array antennas

› State-of-the art: Technology
- Reflector antennas are used but the demands increase
- Arrays are an effective solution, BUT have many elements

› Methodology for sparse array antennas
- No common view on optimum design and best methodology
- No published data on manufactured large arrays

› Focus areas
- Develop an improved methodology
- Investigate important design trade-offs
  - #elements vs. #controls vs. #element types
  - common vs. separated Rx/Tx
- Account for realistic antenna elements and mutual coupling effects

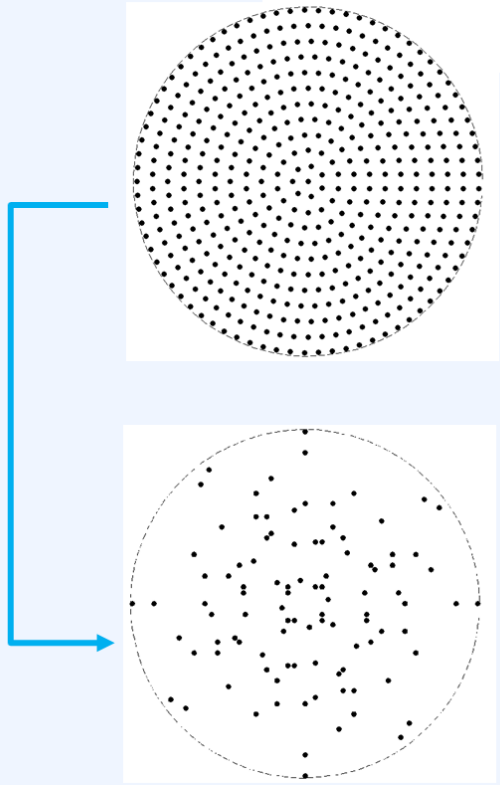

”Chase – the wireless future with Antenna Systems Excellence from CHALMERS”

Array Signal Processing Techniques
+
EM Modeling Approaches

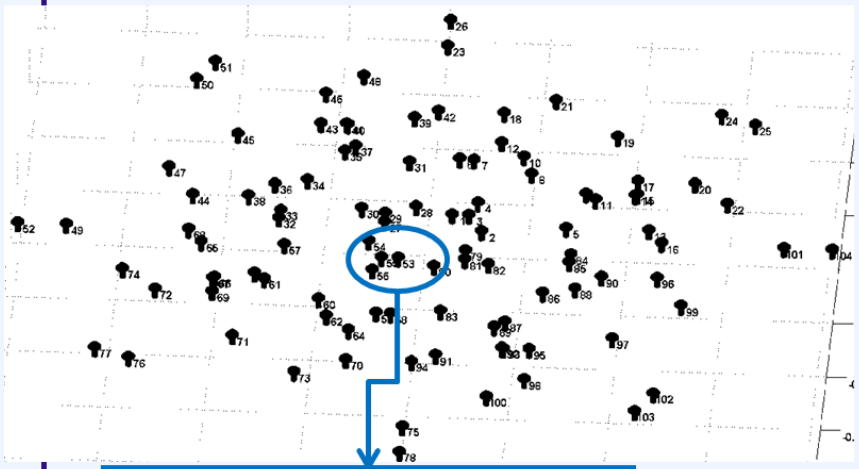

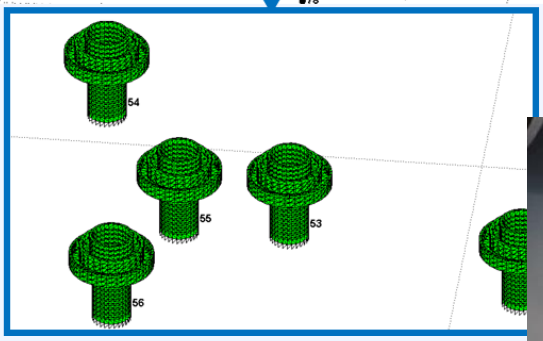

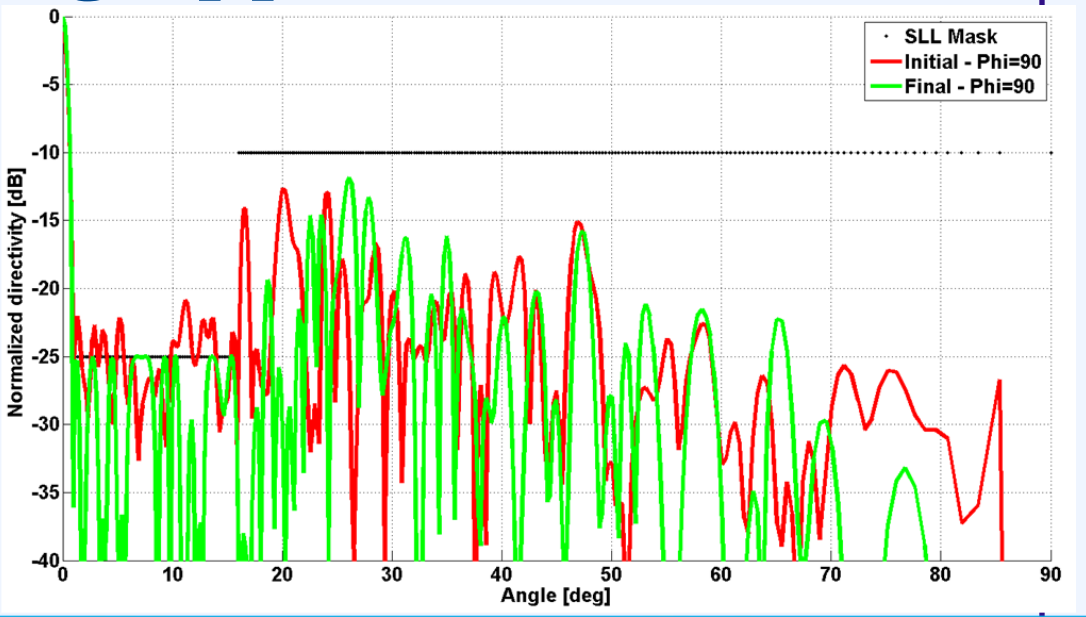

Industrial input, an ideal antenna specification

Frequency band: 17.7-20.2 GHz (TX), 27.5-30.0 GHz (RX)

Dual circular polarization

Coverage: semi-angle 4° (max 8°)

Inter-beam distance 0.5-1°

Cell system: 4 frequency bands in both TX & RX

Edge of Coverage gain to be optimized

Out of coverage gain (SLL): -27dB

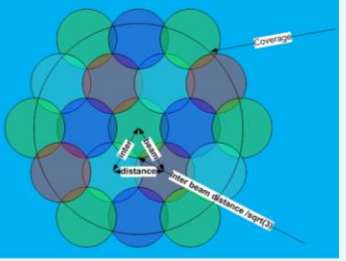

Springer Book Chapter

- Rob Maaskant, “Fast Analysis of Periodic Antennas and Metamaterial-Based Antennas”, Chapter 3, Springer book chapter, pp. 75—109 in *Computational Electromagnetics – Recent Advances and Engineering Applications*, Editor: Raj Mittra, 2013.

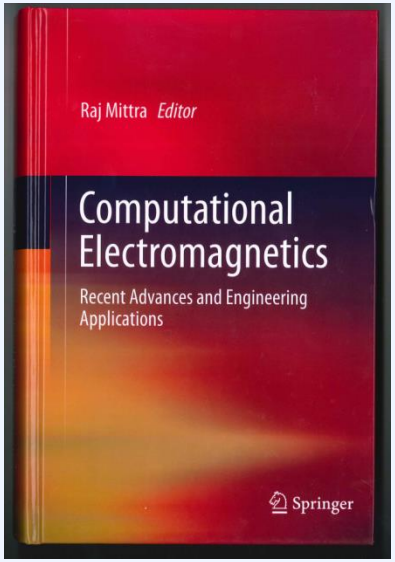

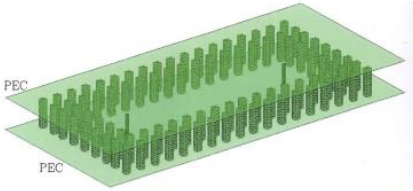

Fig. 3.10 Coaxial-probe excited groove gap waveguide

computationally efficient manner. Furthermore, in Sect. 3.2.1 we observed that the CBFM operates on the matrix equation without requiring knowledge about the specific type of basis functions, integral equation operators, or Green's functions used. For the fast analysis of gap waveguides, we therefore use the CBFM as an enhancement technique for the MoM approach that employs the parallel-plate Green's function [41]. Consequently, we will only need to discretize and solve for the electric currents on the pins and probes in Fig. 3.10.

In regard to the configuration shown in Fig. 3.11, the parallel-plate Green's function computation illustrates that a dipole point source can have an x-, y-, or z-orientation (or linear combinations thereof) inside a parallel-plate region. After application of the image principle, the EM field is regarded as being radiated by two superimposed 1D-line arrays of dipole point sources with the original and possibly mirrored polarization. Each line array has an inter-dipole spacing of twice the plate distance: $2d$. In Dyadic form, the spatial parallel-plate Green's function $\mathbf{G}$ is expressed as $\mathbf{G}(\boldsymbol{r},\boldsymbol{r}') = G_{xx}^N \hat{\boldsymbol{x}}\hat{\boldsymbol{x}}^T + G_{yy}^N \hat{\boldsymbol{y}}\hat{\boldsymbol{y}}^T + G_{zz}^N \hat{\boldsymbol{z}}\hat{\boldsymbol{z}}^T$, where

$$
\begin{aligned}
G_{xx}^N &= \sum_{n=-N}^{N} \frac{e^{-jk_0\sqrt{\rho^2+(z-z'+2dn)^2}}}{4\pi\sqrt{\rho^2+(z-z'+2dn)^2}} \\
&\quad - \sum_{n=-N}^{N} \frac{e^{-jk_0\sqrt{\rho^2+(z+z'+2d(n-1))^2}}}{4\pi\sqrt{\rho^2+(z+z'+2d(n-1))^2}} \\
G_{yy}^N &= G_{xx}^N \\
G_{zz}^N &= \sum_{n=-N}^{N} \frac{e^{-jk_0\sqrt{\rho^2+(z-z'+2dn)^2}}}{4\pi\sqrt{\rho^2+(z-z'+2dn)^2}} \\
&\quad + \sum_{n=-N}^{N} \frac{e^{-jk_0\sqrt{\rho^2+(z+z'+2d(n-1))^2}}}{4\pi\sqrt{\rho^2+(z+z'+2d(n-1))^2}}
\end{aligned}
\tag{3.32}
$$

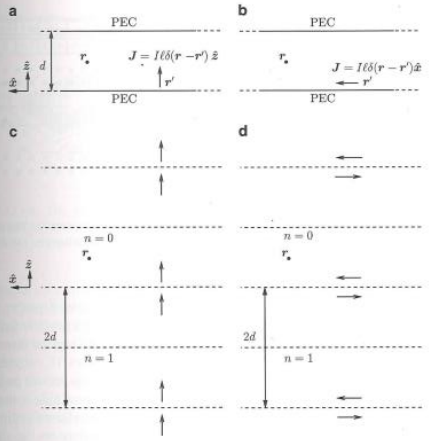

Fig. 3.11 (**a**) z-polarized and (**b**) x-polarized electric Hertzian dipole currents in between two infinitely large parallel PEC plates separated by a distance d; (**c**) and (**d**), the repeated application of the image principle for both dipole polarizations, respectively

for $N \to \infty$, and where $\rho^2 = (x-x')^2 + (y-y')^2$. The spatial summations in Eq. (3.32) are known to be slowly convergent, however, each summation can be computed rapidly using the Shanks transformation [37]. This method is easy to implement and very fast if only a few digits of accuracy is required, which is sufficient in most practical cases [41]. For example, when considering the new series $G_{xx}^1, G_{xx}^2, \ldots$, the Shanks-extrapolated value for G_{xx}^∞ is

$$
G_{xx}^\infty \approx \frac{G_{xx}^{N+1}G_{xx}^{N-1} - \left(G_{xx}^N\right)^2}{G_{xx}^{N+1} - 2G_{xx}^N + G_{xx}^{N-1}} \tag{3.33}
$$

where N is taken sufficiently large. Numerical experiments show that the best trade-off between the solution accuracy and the total series evaluation time is to use the doubly repeated Shanks transformation, which only requires $N \approx 5$ terms [41].

The electric surface currents on the pins and coaxial probes, of the guiding structure shown in Fig. 3.10, are expanded in terms of 37088 RWG basis functions.

W_{pin}	H_{pin}	L_1	L_2	L_3	L_4
1	6.25	15.8	43.7	5.4	2

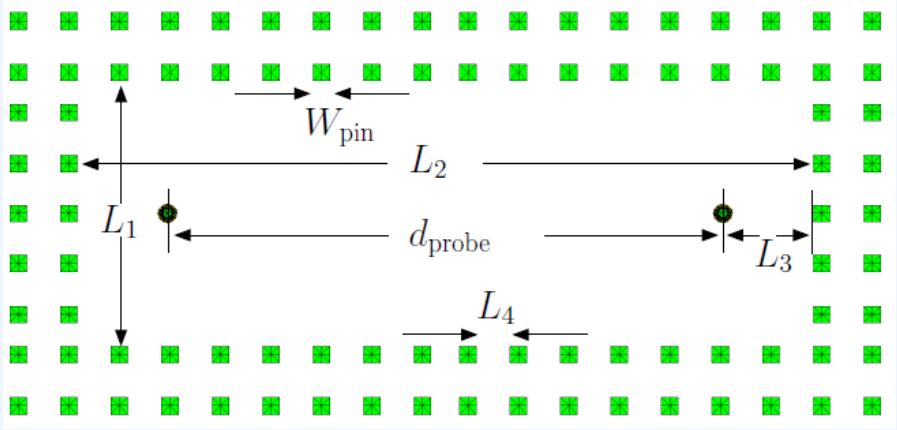

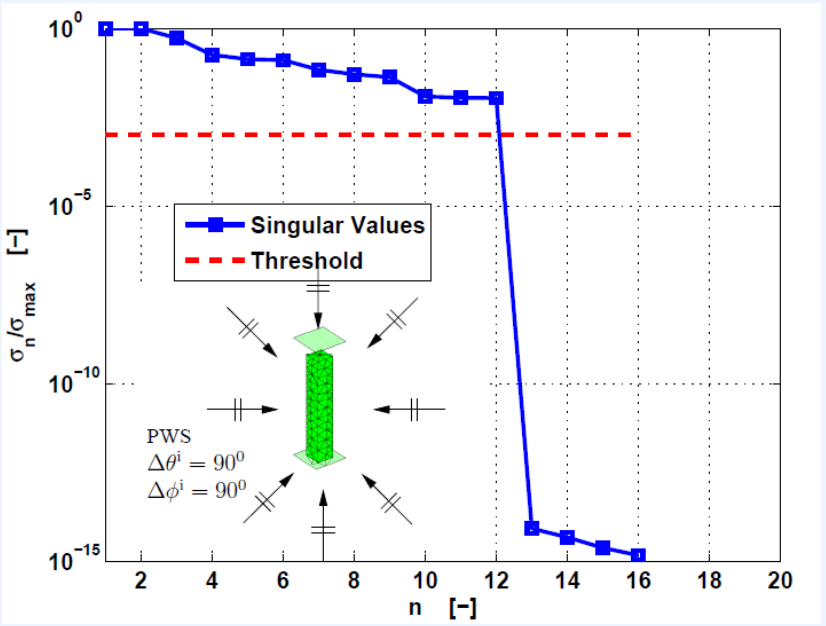

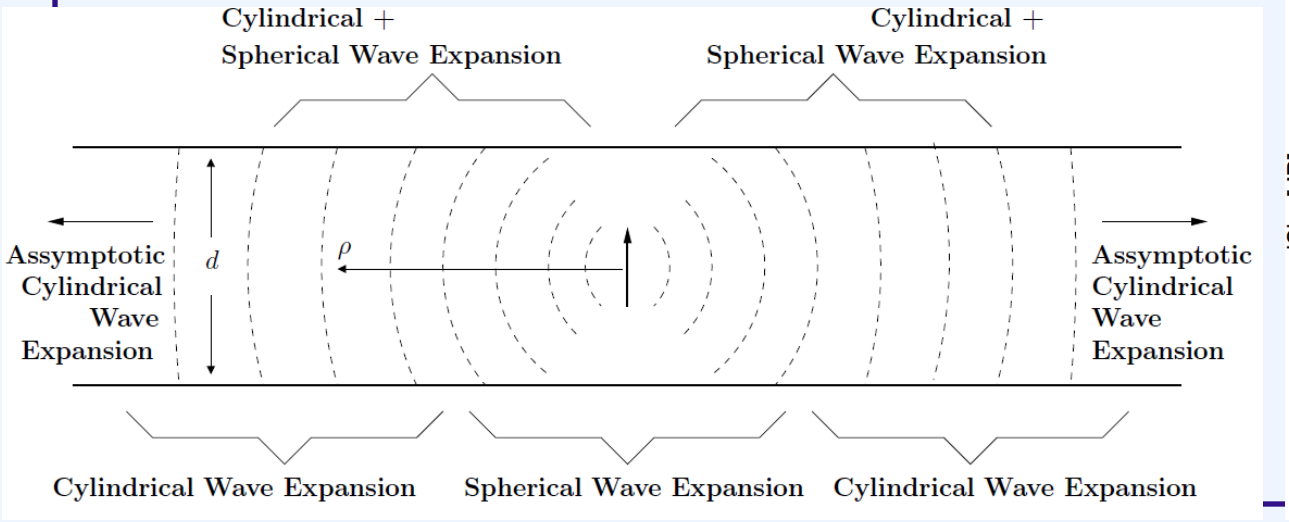

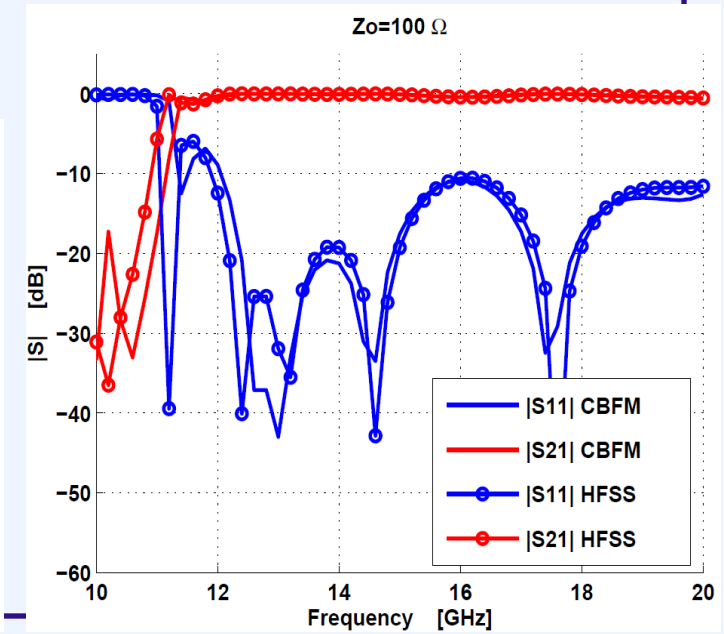

Springer Book Chapter

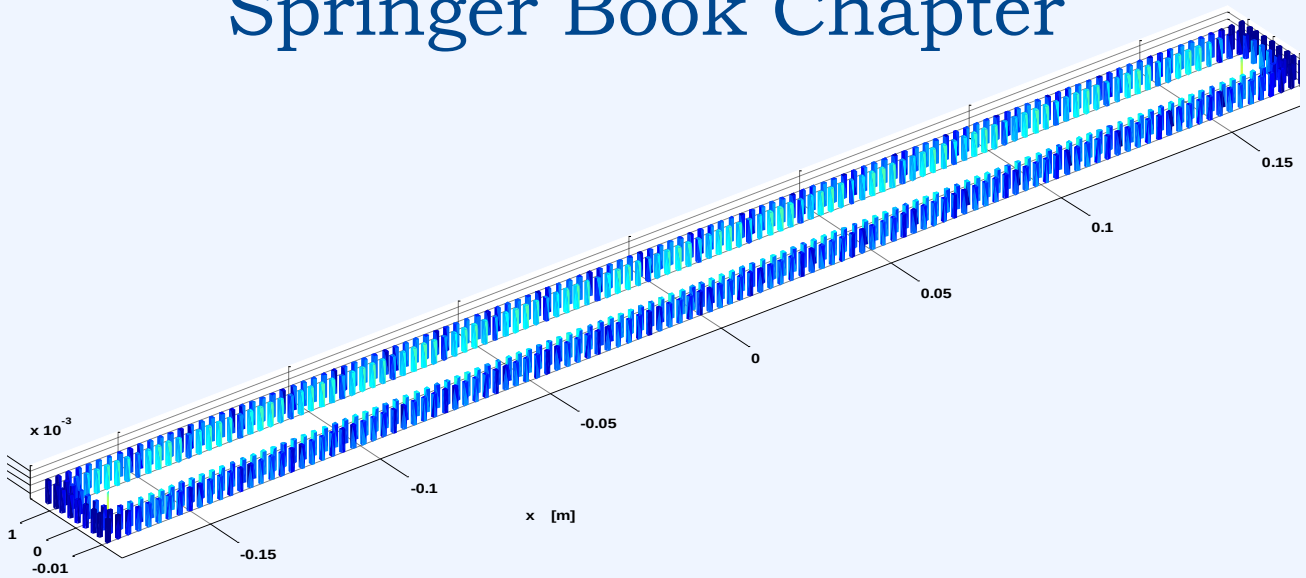

A slightly larger problem, though still easily solvable:

	CAESAR	**HFSS** **(13 mesh refinement steps, 1% port accuracy)**
Meshing time:	7 sec.	13th pass: 1 min. 9 sec.
MoM matrix fill + equation solving	2 min. 24 sec.	3 min. 53 sec.
# Mesh cells	28620 RWGs (5912 CBFs)	155845 tetrahedra

Note: the max. number of CBFs that can be handled is about 30000

Springer Book Chapter

W_{pin}	H_{pin}	L_1	L_2	L_3	L_4
1	6.25	15.8	43.7	5.4	2

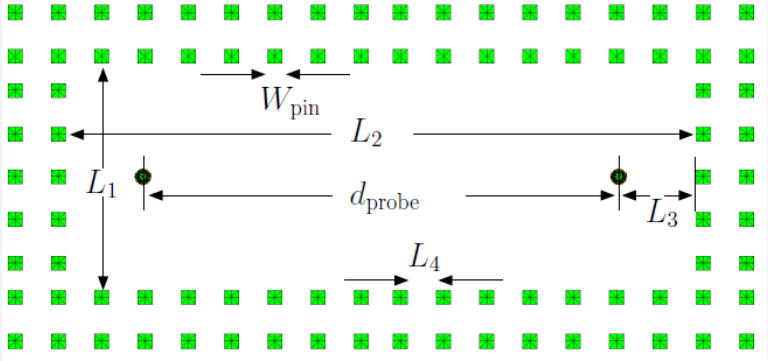

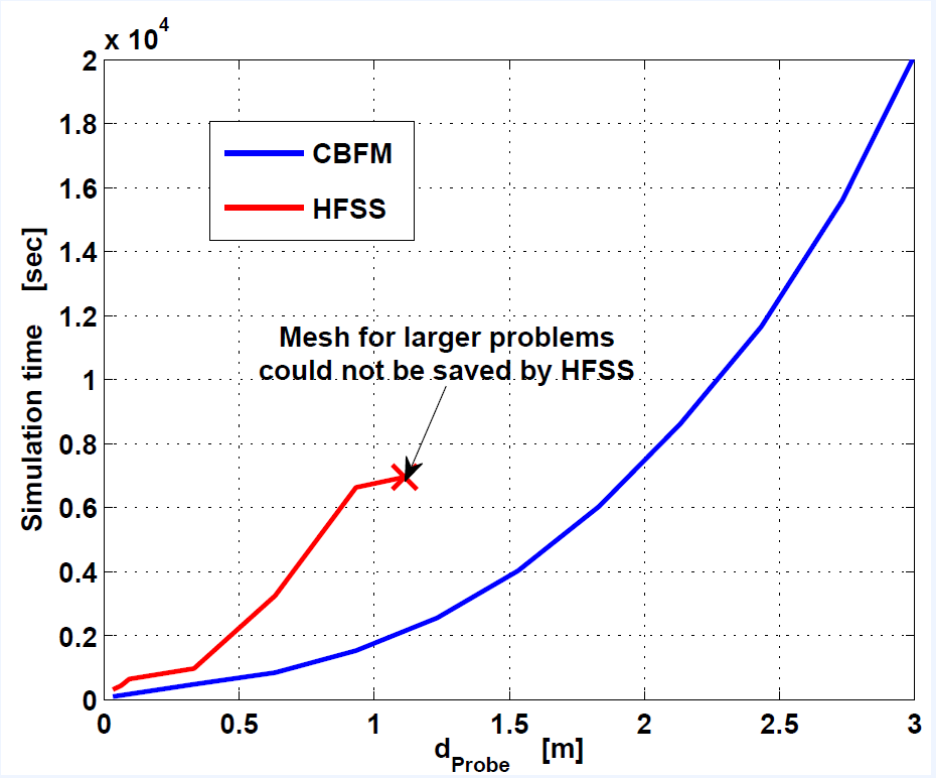

Simulation time vs. Problem Size

Current Modeling Capabilities of CAESAR

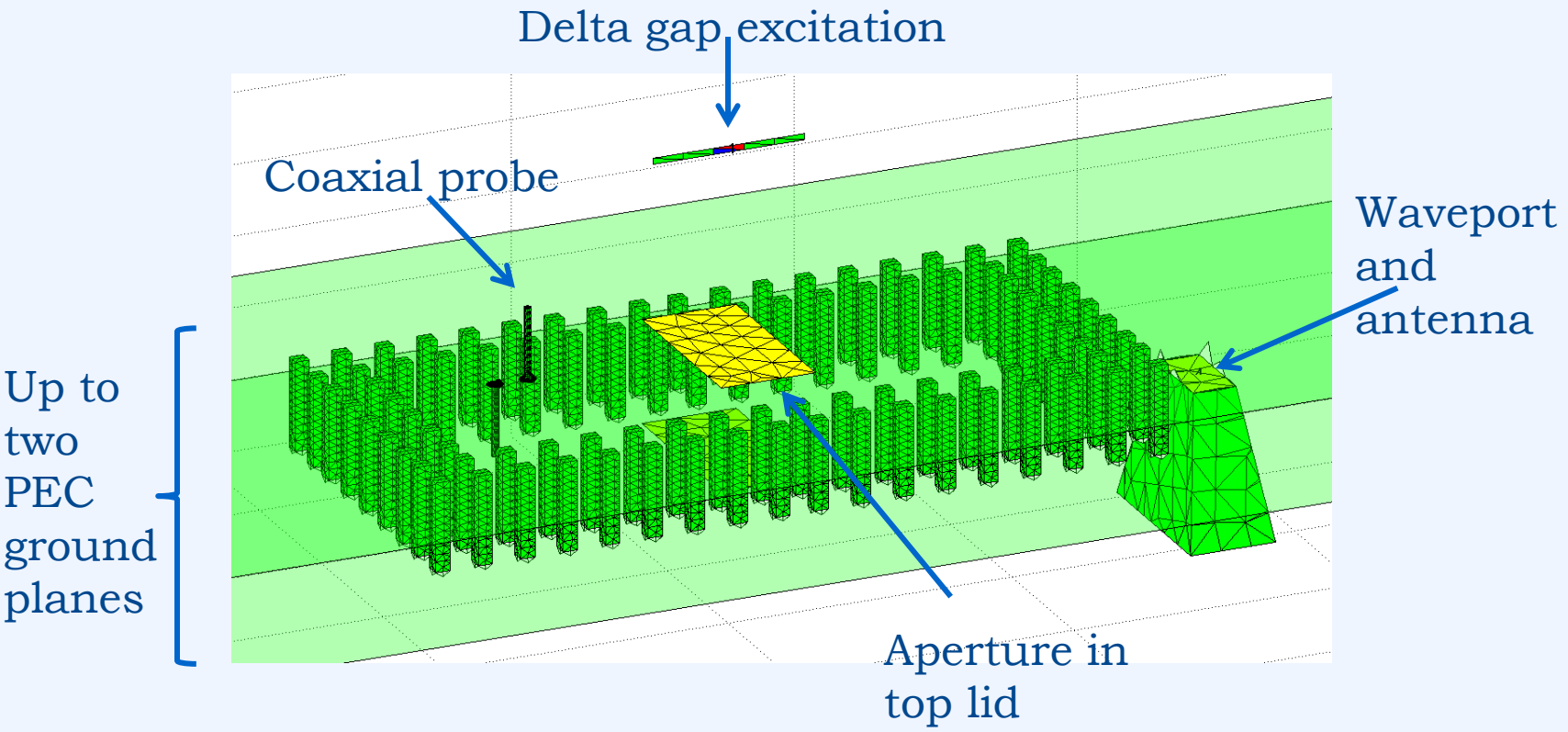

- Shanks transformation accelerated Parallel Plate Green's function
- Multi-threaded Characteristic Basis Function Method (CBFM) in each region
- Array structures are computationally exploited using symmetries
- Adaptive Cross Approximation (ACA) algorithm

Generalized Admittance Matrix Approach

Microstrip-Excited Slot Antenna

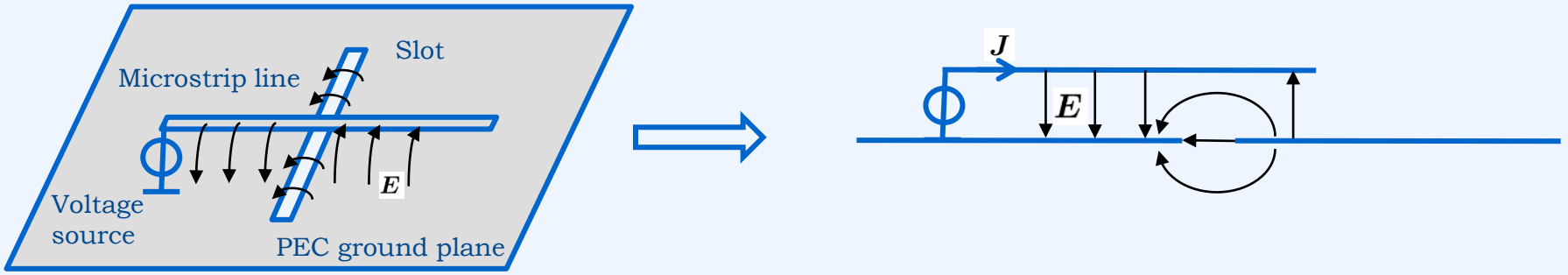

Generalized Admittance Matrix Approach

Microstrip-Excited Slot Antenna

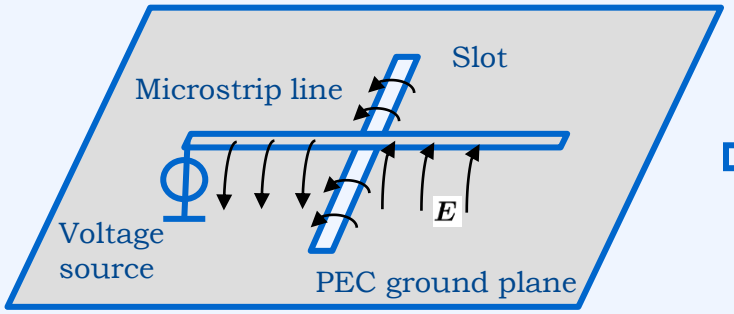

Above PEC ground plane

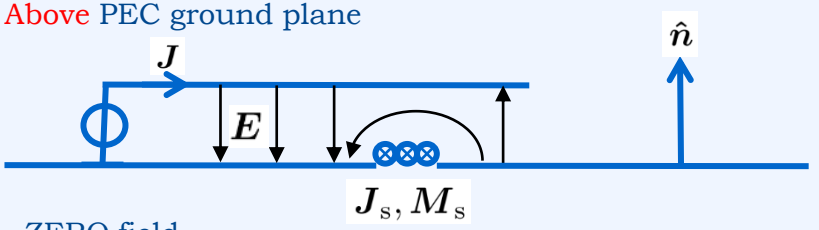

ZERO field

Boundary conditions at the slot

$$\begin{cases} \boldsymbol{J}_s = \hat{\boldsymbol{n}} \times \boldsymbol{H} \\ \boldsymbol{M}_s = -\hat{\boldsymbol{n}} \times \boldsymbol{E} \end{cases}$$

Above PEC ground plane

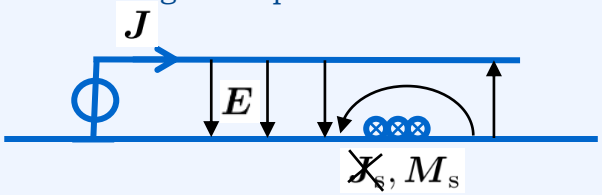

ZERO field

ZERO field

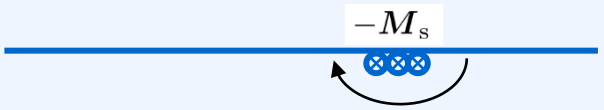

Below PEC ground plane

Generalized Admittance Matrix Approach

Above PEC ground plane

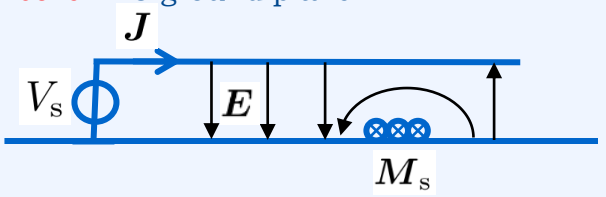

ZERO field

Discretization $\boldsymbol{M}_{\mathrm{s}}(\boldsymbol{r}) = \sum_{n=1}^{N_{\mathrm{M}}} V_n \boldsymbol{f}_n^{\mathrm{M}}(\boldsymbol{r})$

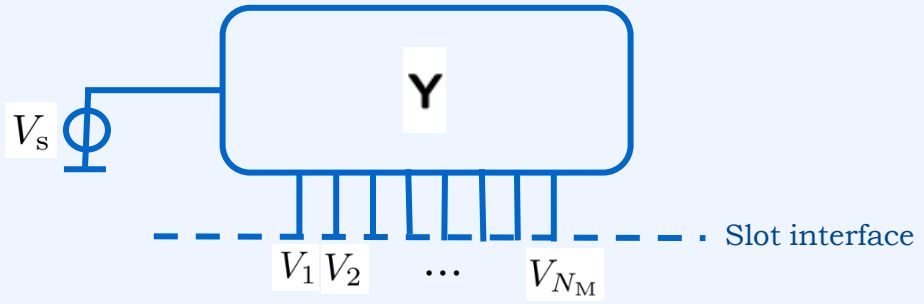

Mutual Admittance $Y_{mn} = -\frac{1}{V_m V_n} \iint \boldsymbol{M}_m \cdot \boldsymbol{H}_n \, \mathrm{d}S$

$V_m = V_n = 1$

$Y_{mn} = -\iint \boldsymbol{f}_m^{\mathrm{M}} \cdot \left[\boldsymbol{H}(\boldsymbol{f}_n^{\mathrm{M}}) + \boldsymbol{H}(\boldsymbol{J}) \right] \mathrm{d}S$

EFIE solution

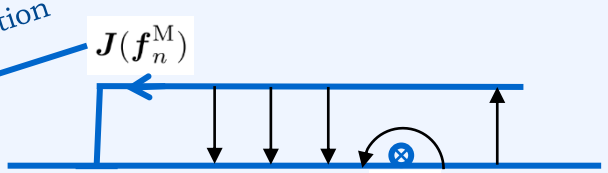

Source $\boldsymbol{f}_n^{\mathrm{M}}$ generating incident E-field

Generalized Admittance Matrix Approach

Microstrip-Excited Slot Antenna

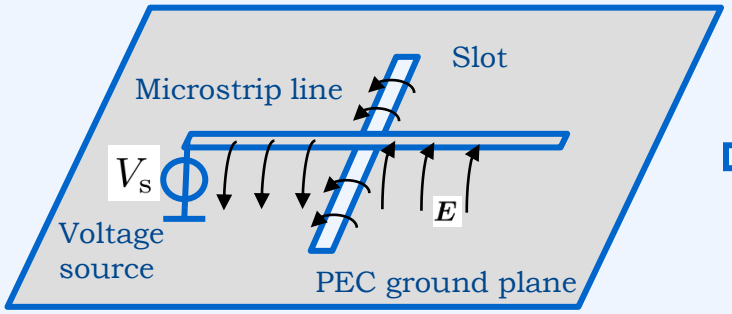

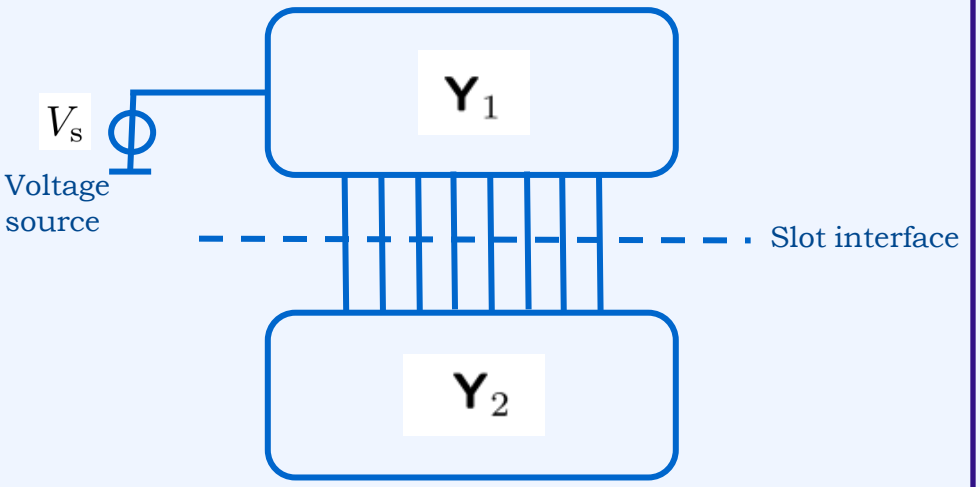

Solving a network problem !!

- After port currents and voltages are known, all currents are known
- Antenna radiation and impedance characteristics can be computed

Connection Matrix Theory

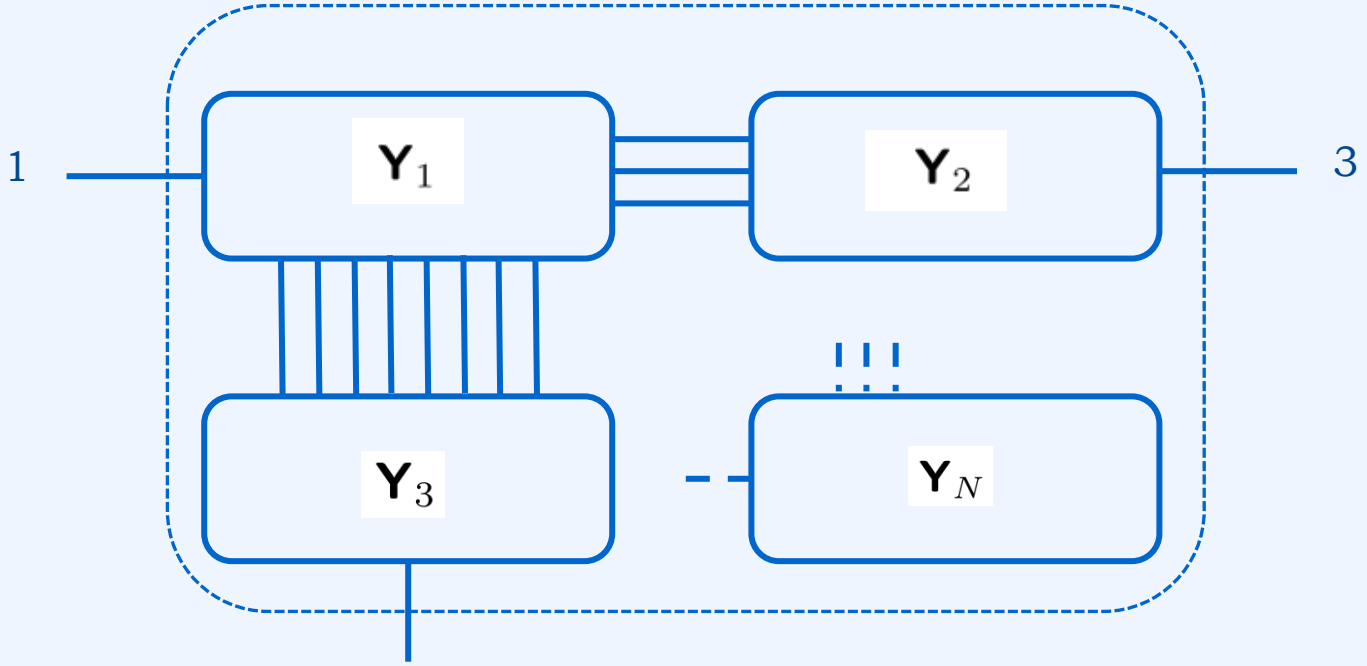

$$\begin{bmatrix} \mathbf{Y}_1 & \mathbf{0} & \mathbf{0} & \mathbf{0} \\ \mathbf{0} & \mathbf{Y}_2 & \mathbf{0} & \mathbf{0} \\ \mathbf{0} & \mathbf{0} & \ddots & \mathbf{0} \\ \mathbf{0} & \mathbf{0} & \mathbf{0} & \mathbf{Y}_N \end{bmatrix} \begin{bmatrix} \mathbf{V}_1 \\ \mathbf{V}_2 \\ \vdots \\ \mathbf{V}_N \end{bmatrix} = \begin{bmatrix} \mathbf{I}_1 \\ \mathbf{I}_2 \\ \vdots \\ \mathbf{I}_N \end{bmatrix}$$

Sparse Matrix

Connection Matrix Theory

$$\begin{bmatrix} \mathbf{Y}_1 & \mathbf{0} & \mathbf{0} & \mathbf{0} \\ \mathbf{0} & \mathbf{Y}_2 & \mathbf{0} & \mathbf{0} \\ \mathbf{0} & \mathbf{0} & \ddots & \mathbf{0} \\ \mathbf{0} & \mathbf{0} & \mathbf{0} & \mathbf{Y}_N \end{bmatrix} \begin{bmatrix} \mathbf{V}_1 \\ \mathbf{V}_2 \\ \vdots \\ \mathbf{V}_N \end{bmatrix} = \begin{bmatrix} \mathbf{I}_1 \\ \mathbf{I}_2 \\ \vdots \\ \mathbf{I}_N \end{bmatrix}$$

Rearrange to separate between internal and external ports

$$\begin{bmatrix} \mathbf{Y}_{ii} & \mathbf{Y}_{ie} \\ \mathbf{Y}_{ei} & \mathbf{Y}_{ee} \end{bmatrix} \begin{bmatrix} \mathbf{V}_i \\ \mathbf{V}_e \end{bmatrix} = \begin{bmatrix} \mathbf{I}_i \\ \mathbf{I}_e \end{bmatrix}$$

Accordingly,

(1) $\mathbf{Y}_{ii}\mathbf{V}_i + \mathbf{Y}_{ie}\mathbf{V}_e = \mathbf{I}_i$

(2) $\mathbf{Y}_{ei}\mathbf{V}_i + \mathbf{Y}_{ee}\mathbf{V}_e = \mathbf{I}_e$

(3) $\mathbf{V}_i = \mathbf{\Gamma}\mathbf{V}_i$

(4) $\mathbf{I}_i = -\mathbf{\Gamma}\mathbf{I}_i$

Internal port connections

Connection matrix containing ones and zeros

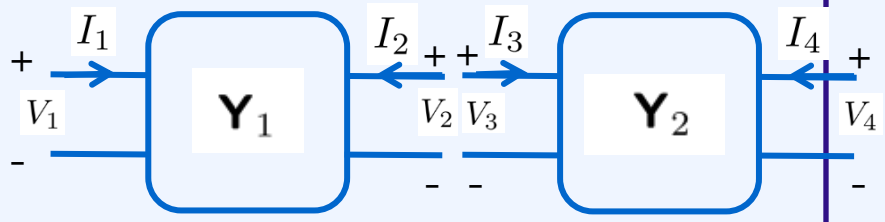

$$\begin{bmatrix} V_2 \\ V_3 \end{bmatrix} = \begin{bmatrix} 0 & 1 \\ 1 & 0 \end{bmatrix} \begin{bmatrix} V_2 \\ V_3 \end{bmatrix}$$

$$\begin{bmatrix} I_2 \\ I_3 \end{bmatrix} = -\begin{bmatrix} 0 & 1 \\ 1 & 0 \end{bmatrix} \begin{bmatrix} I_2 \\ I_3 \end{bmatrix}$$

Connection Matrix Theory

(1) $\mathbf{Y}_{ii}\mathbf{V}_i + \mathbf{Y}_{ie}\mathbf{V}_e = \mathbf{I}_i$

(2) $\mathbf{Y}_{ei}\mathbf{V}_i + \mathbf{Y}_{ee}\mathbf{V}_e = \mathbf{I}_e$

(3) $\mathbf{V}_i = \boldsymbol{\Gamma}\mathbf{V}_i$

(4) $\mathbf{I}_i = -\boldsymbol{\Gamma}\mathbf{I}_i$

(3) and (4) in (1): $\mathbf{Y}_{ii}\boldsymbol{\Gamma}\mathbf{V}_i + \mathbf{Y}_{ie}\mathbf{V}_e = -\boldsymbol{\Gamma}\mathbf{I}_i$

$\boldsymbol{\Gamma}\times$ (1): $\boldsymbol{\Gamma}\mathbf{Y}_{ii} + \boldsymbol{\Gamma}\mathbf{Y}_{ie}\mathbf{V}_e = +\boldsymbol{\Gamma}\mathbf{I}_i$

+

$$\mathbf{V}_i = -\left(\boldsymbol{\Gamma}\mathbf{Y}_{ii} + \mathbf{Y}_{ii}\boldsymbol{\Gamma}\right)^{-1}\left(\mathbf{I} + \boldsymbol{\Gamma}\right)\mathbf{Y}_{ie}\mathbf{V}_e$$

$$\mathbf{W} = -\left(\boldsymbol{\Gamma}\mathbf{Y}_{ii} + \mathbf{Y}_{ii}\boldsymbol{\Gamma}\right)^{-1}\left(\mathbf{I} + \boldsymbol{\Gamma}\right)$$

(5) $\mathbf{V}_i = \mathbf{W}\mathbf{Y}_{ie}\mathbf{V}_e$

(5) In (2) : $\left[\mathbf{Y}_{ee} + \mathbf{Y}_{ei}\mathbf{W}\mathbf{Y}_{ie}\right]\mathbf{V}_e = \mathbf{I}_e$

$$\mathbf{Y}_{tot} = \mathbf{Y}_{ee} + \mathbf{Y}_{ei}\mathbf{W}\mathbf{Y}_{ie}$$

Generalized Admittance Matrix Approach

Microstrip-Excited Slot Antenna

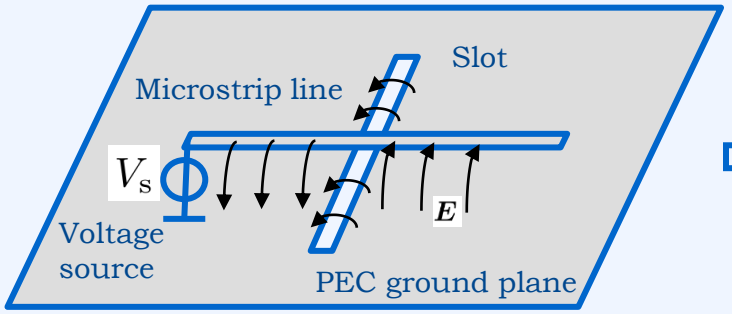

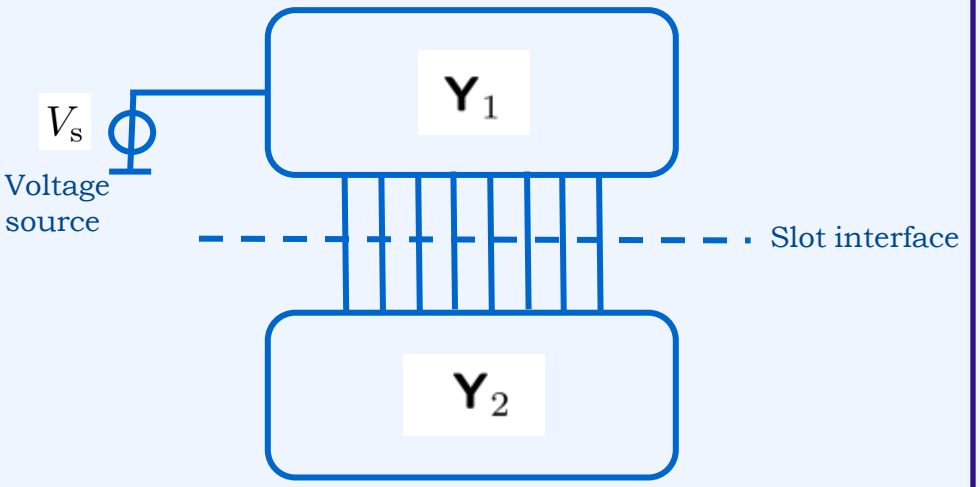

Solving a network problem !!

- After port currents and voltages are known, all currents are known
- Antenna radiation and impedance characteristics can be computed

Numerical Examples

Waveport-Excited Aperture Antenna Array

Credits: PhD student Carlo Bencivenni (NGAA Chase project)

TE11 mode

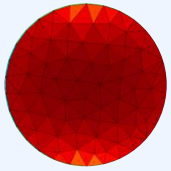

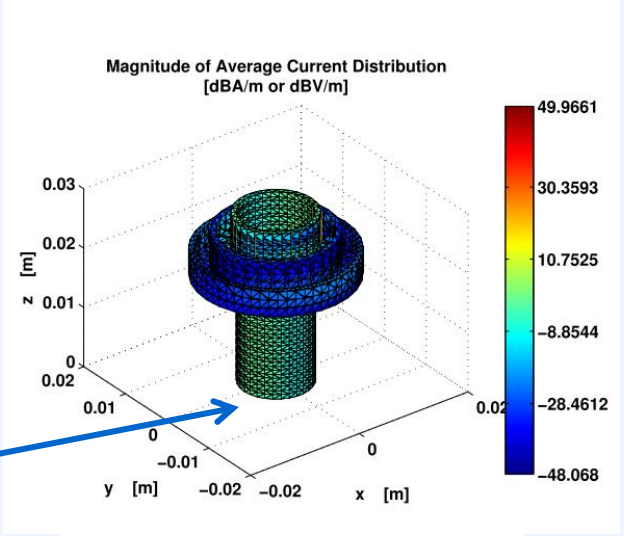

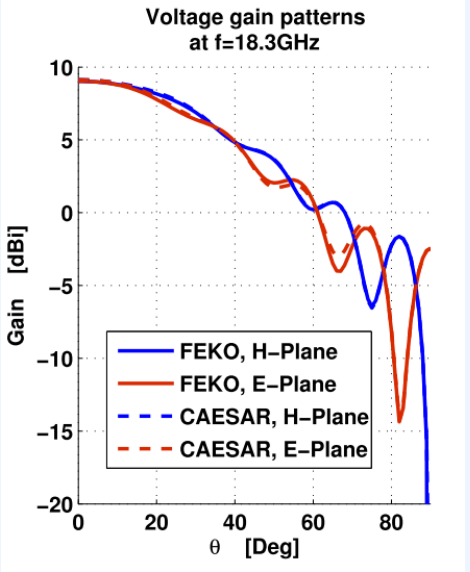

~3,000,000 RWG basis functions!

(2014 EuCAP paper)

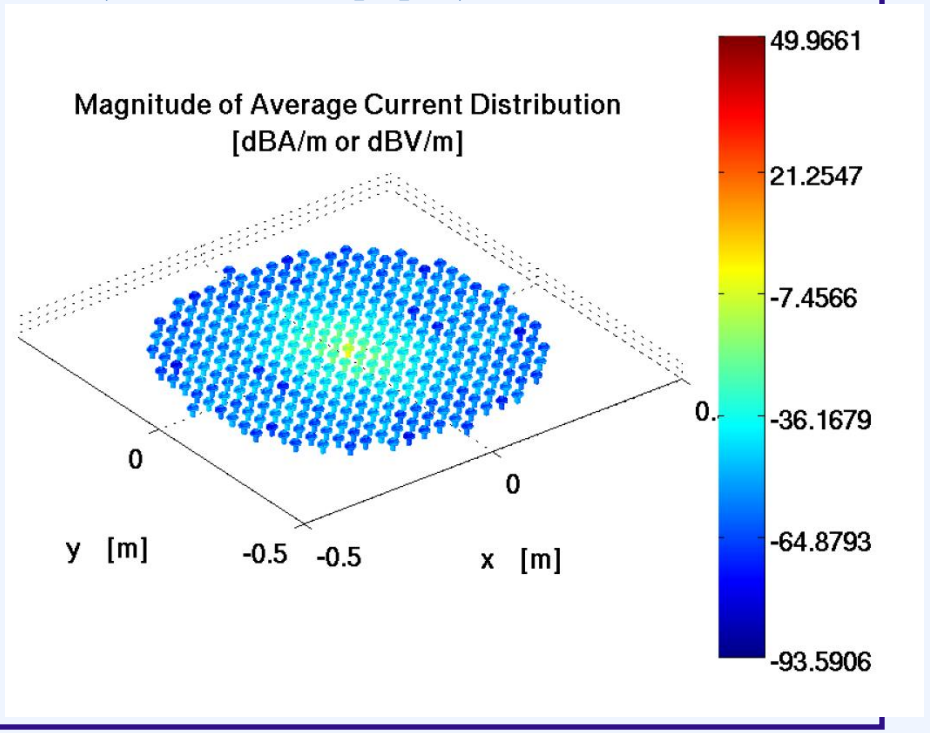

Microstrip-Excited Slot Antenna

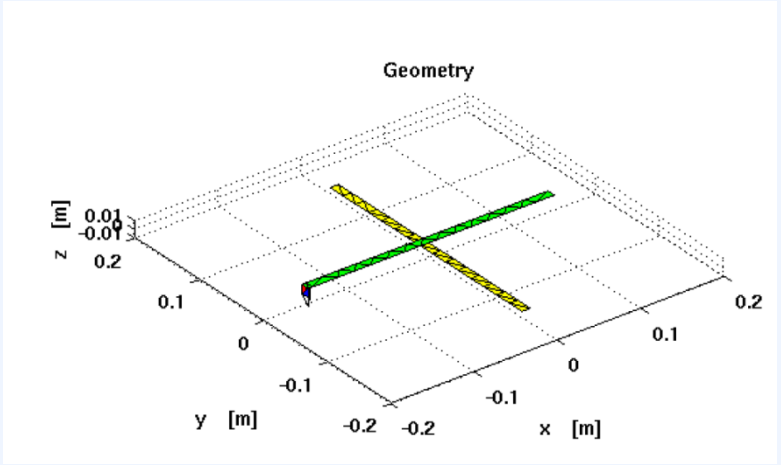

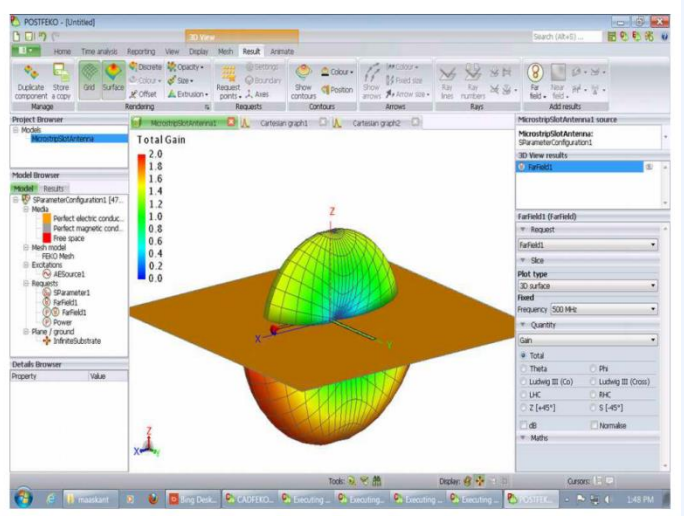

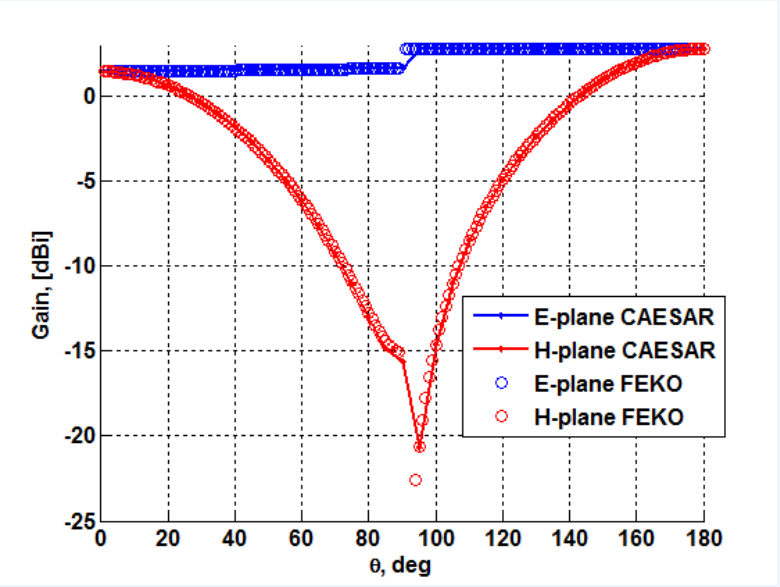

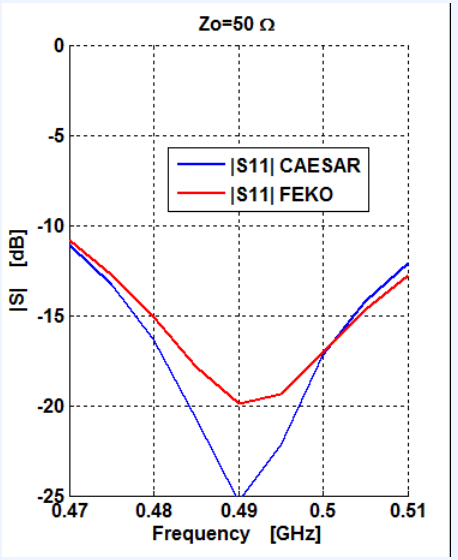

Stripline-Excited Bilateral Slot Antenna

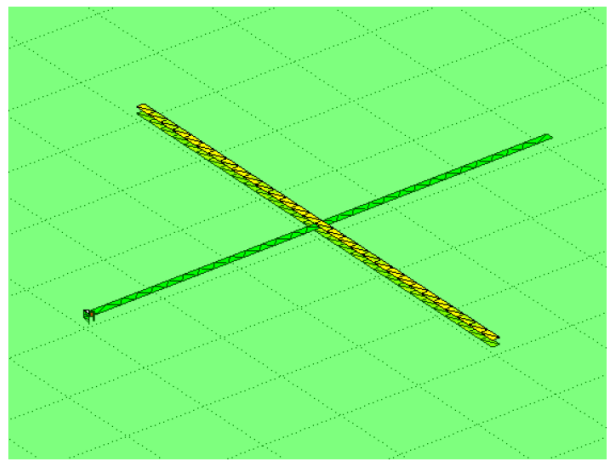

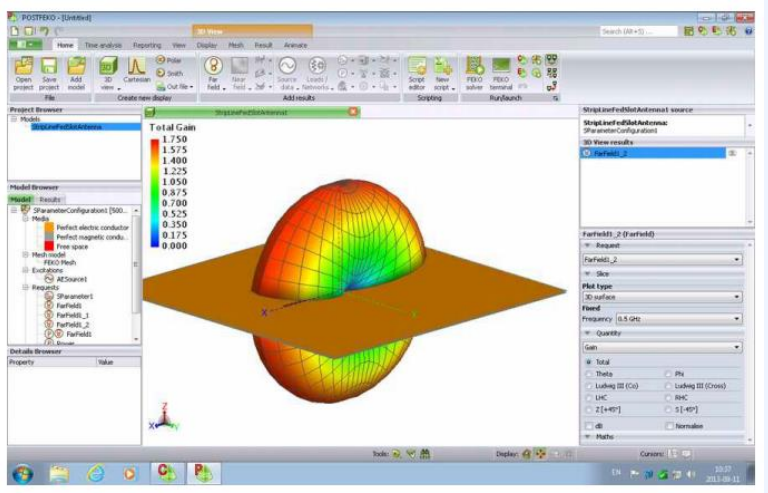

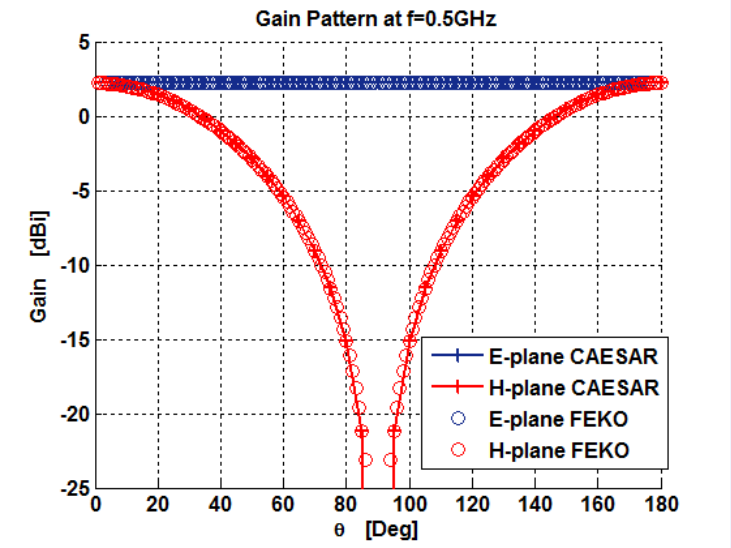

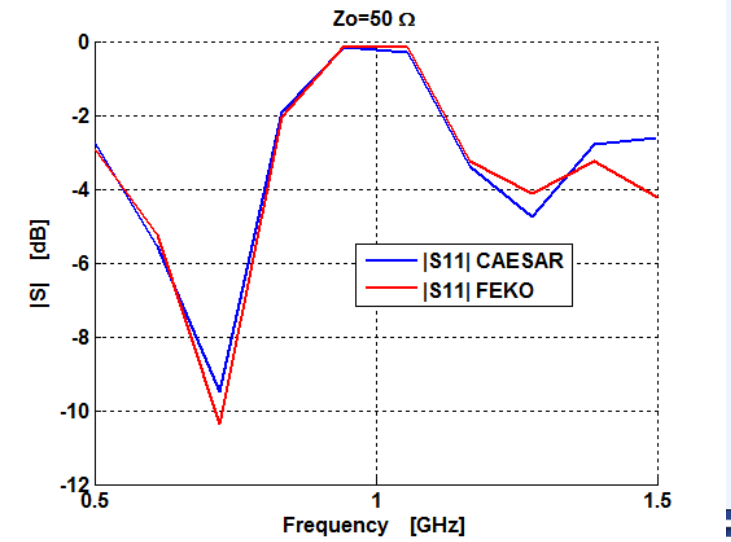

Solution for a large sparse array

Aperture diameter 100λ

Final array design with 96 elements

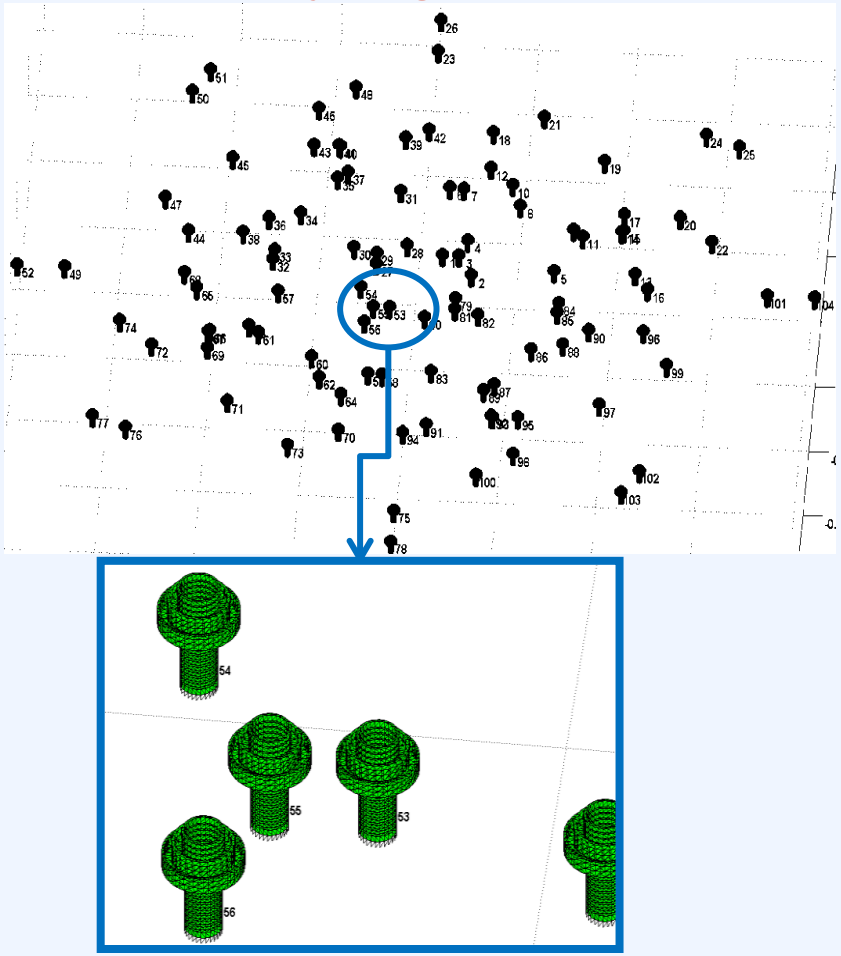

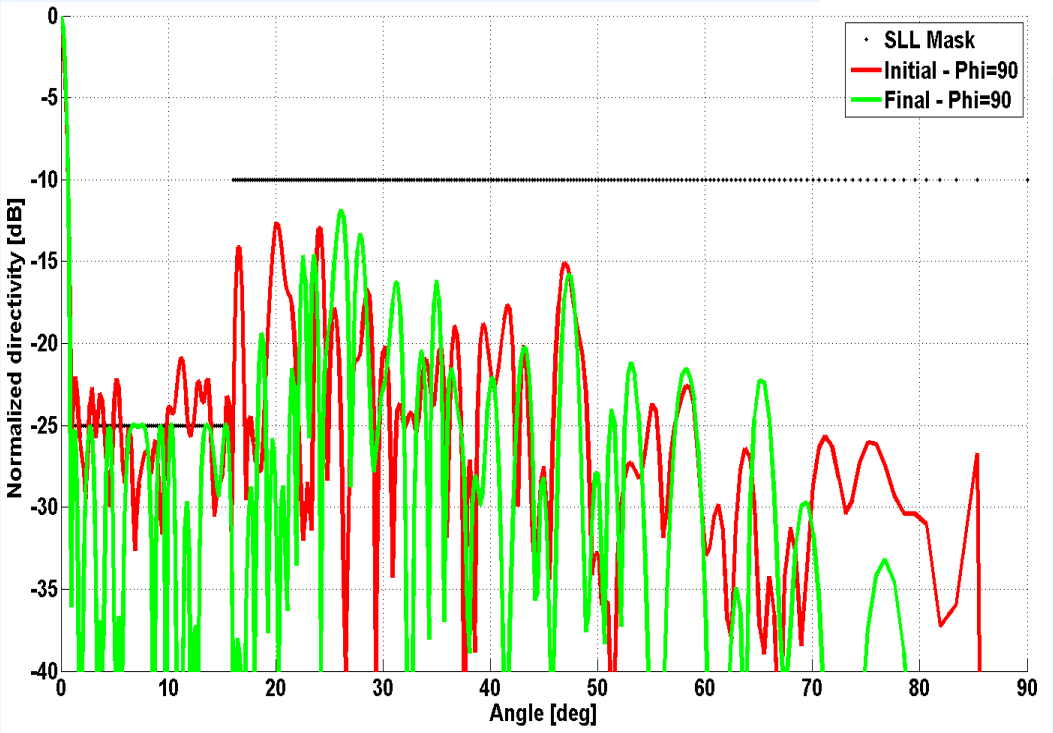

	Simulation time
ℓ_1-norm algorithm per iteration	4½ hours
~1k CBFs (~200k RWGs) per iteration	1½ hours
Total time for the combined ℓ_1-norm CBFM:	1.5 day

”Chase – the wireless future with Antenna Systems Excellence from CHALMERS”

Coaxial-Probe-Excited Ridge Gap Waveguide Antenna

CST: Dr. Ashraf Uz Zaman

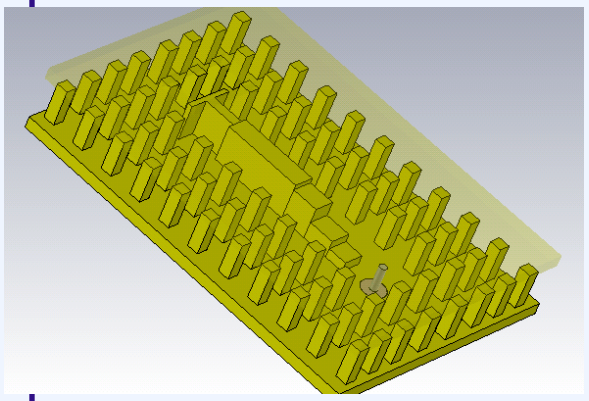

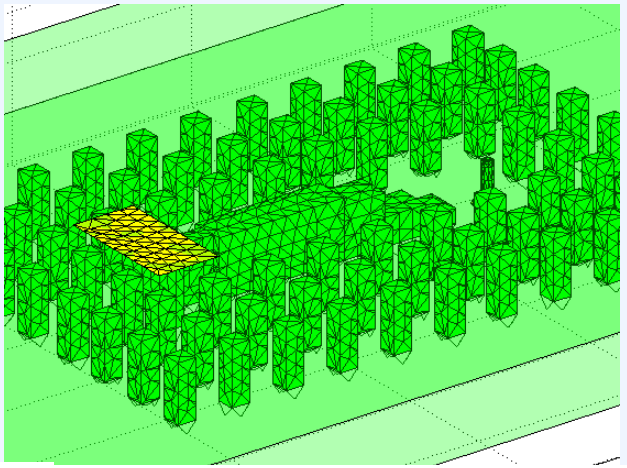

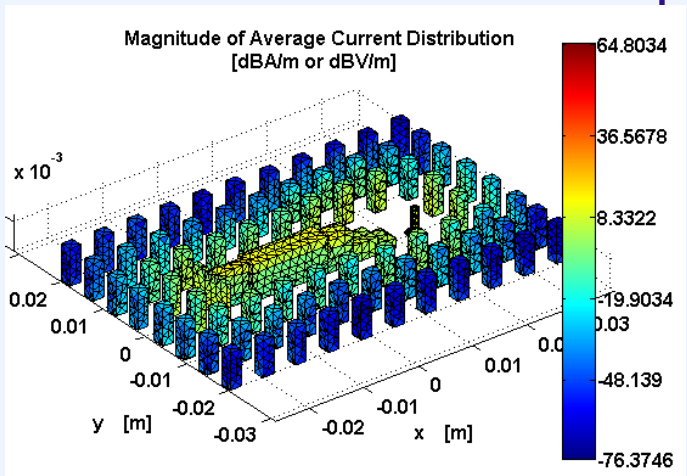

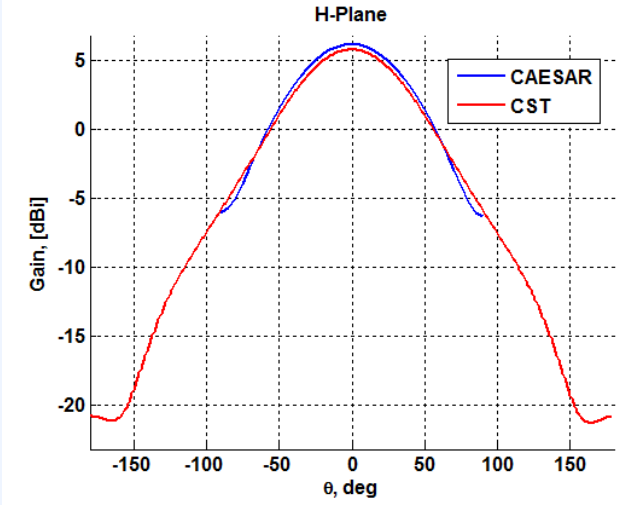

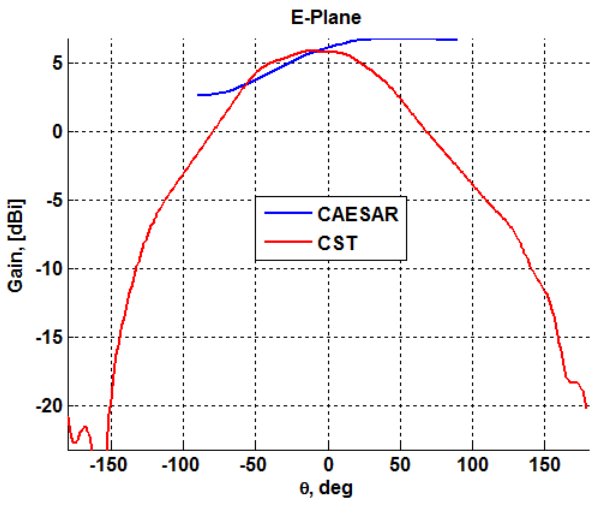

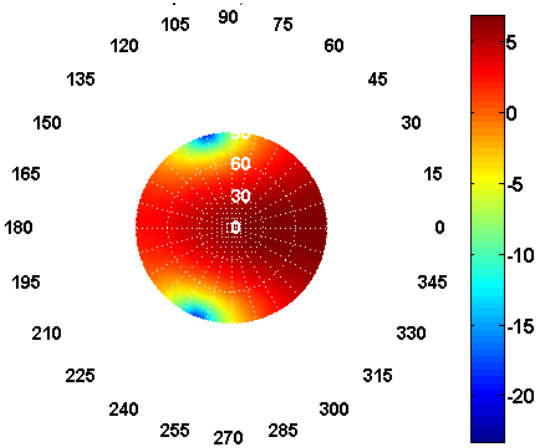

Short-Circuited Slot

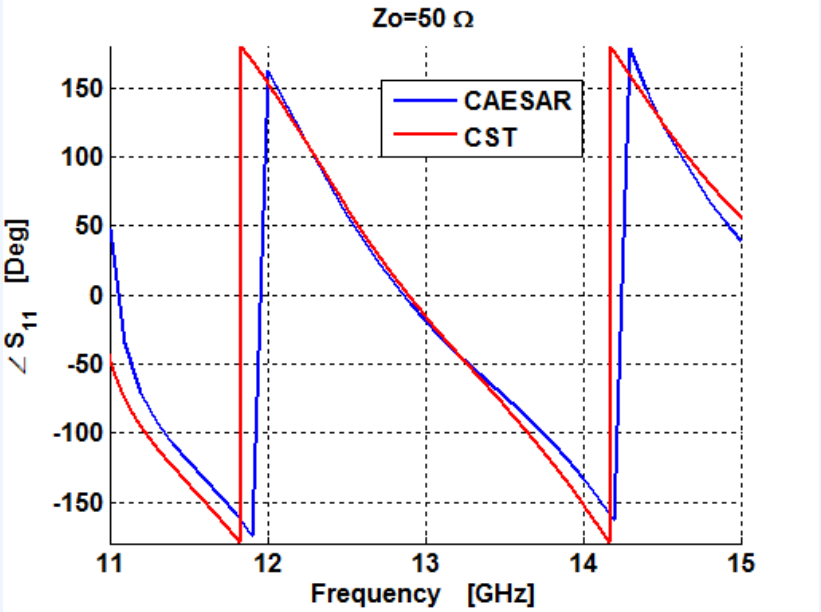

Back-to-back

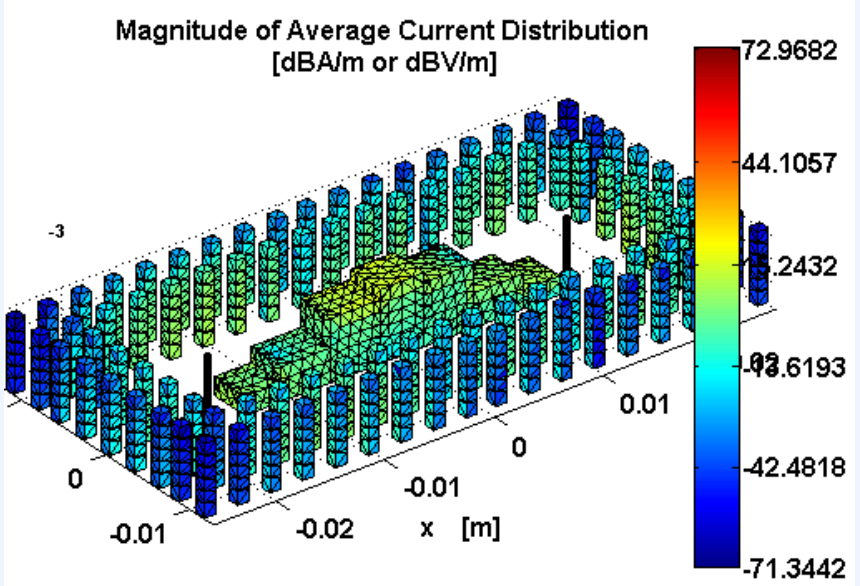

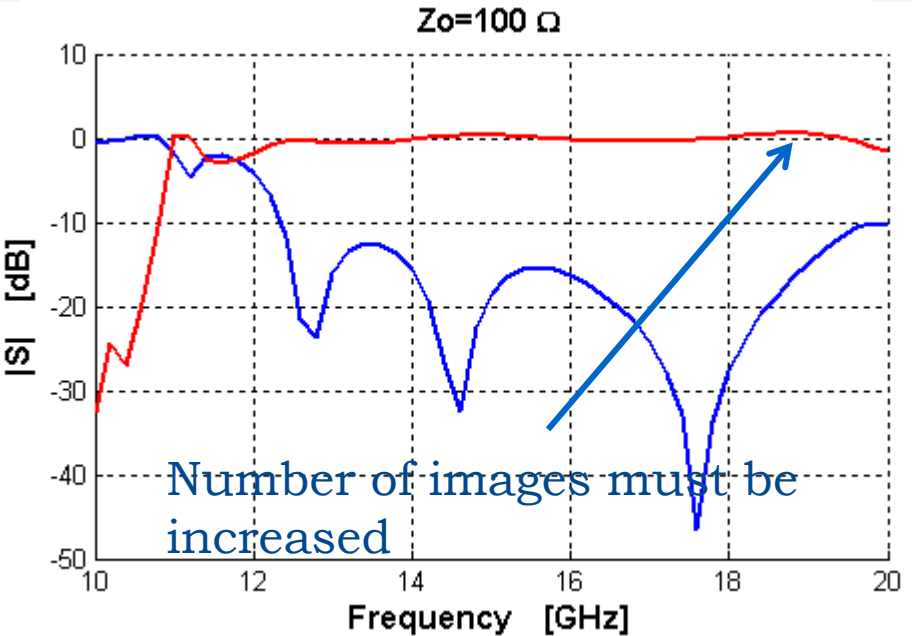

Conclusions and Outlook

- Generalized Admittance Matrix Approach implemented + CBFM applied to three layers
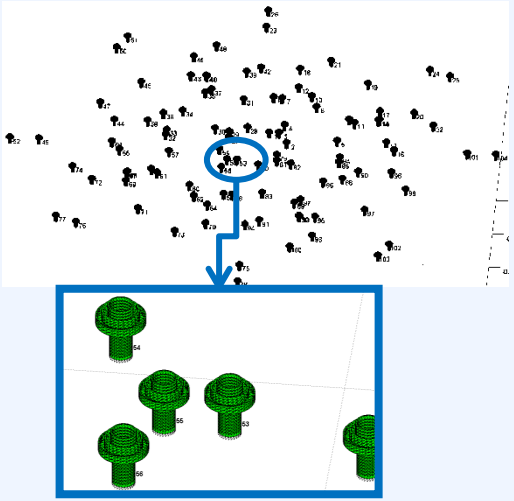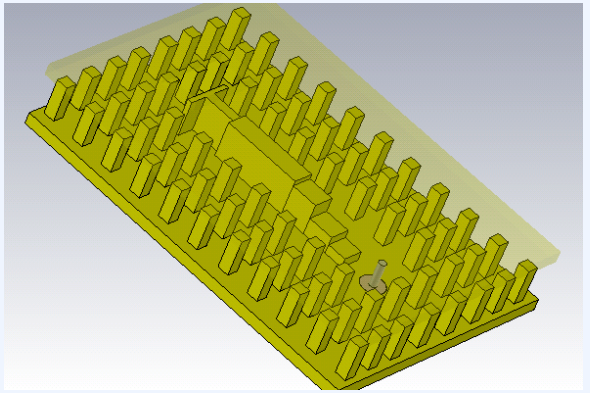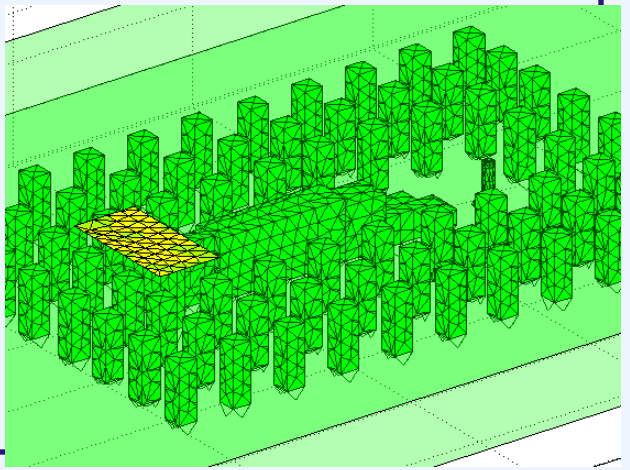
- Method Enables the Analysis of Large Aperture-Fed Antenna Arrays
  - Irregular Antenna Arrays (ongoing – to be published)
  - Gap Waveguide Antennas (ongoing – to be published)